Sustainable Development and Innovations in Marine Technologies – Georgiev & Guedes Soares (eds)
© 2020 Taylor & Francis Group, London, ISBN 978-0-367-40951-7

An investigation into the effect of the Hull Vane on the ship resistance in OpenFOAM

C. Celik & D.B. Danisman
Department of Naval Architecture and Ocean Engineering, Istanbul Technical University, Istanbul, Turkey

P. Kaklis & S. Khan
Department of Naval Architecture, Ocean & Marine Engineering, University of Strathclyde, Glasgow, UK

ABSTRACT: The patented Hull Vane, the energy saving appendage, is used to reduce the power need of the ships. It is a hydrofoil wing transversely fixed at the transom bottom of the ships. A negative pressure zone, which helps to reduce the stern wave, appears on the suction side of the Hull Vane due to the accelerated flow from the aft of the hull. In this study, the effect of the Hull Vane on the resistance components of the ship has been investigated in detail on the model scale by performing computational fluid dynamics (CFD) simulations. OpenFOAM (Open source Field Operation and Manipulation) has been used as a flow solver which is able to solve different types of fluid dynamics problems. In the scope of the numerical study the chord length of the Hull Vane has been changed to examine its effect on the total resistance. A significant 22.9% reduction on the total resistance has been observed on the subject ship as the result of the study.

1 INTRODUCTION

The awareness of reducing carbon emissions has been dramatically increasing. The new restrictive regulations about carbon emissions will be implemented by the International Maritime Organization (IMO) in the next years. Therefore, over the last decade, significant attention has been given to reduce fuel consumption. Fuel consumption of a ship can be decreased by employing various techniques such as using alternative energy sources, decreasing the ship hull resistance or increasing the efficiency of its machinery. This study is focused on reducing the ship hull resistance by applying an energy saving device.

Uithof et al. (2014) describe the working principles of the Hull Vane. The principles related to each other are thrust force, trim correction, wave reduction behind the vessel and motion reduction in waves. When the horizontal component of the lift force is greater than the horizontal component of the drag force, the resulting horizontal force provides an additional thrust force. Also, the resulting vertical force affects the total resistance of the vessel by reducing the vessel trim. A negative pressure zone, which helps to reduce the stern wave, appears on the top side of the Hull Vane due to the accelerated flow from the aft geometry of the hull. The Hull Vane damps the pitch and heave motions of the vessel and therefore reduces the added resistance in rough sea conditions. Hull Vane was first tested under the ship's hull. The negative pressure zone on the Hull Vane interacted with the ship's hull, resulted in an additional pressure resistance on the hull. For this reason, it was decided to fit the Hull Vane behind the transom of the ship. Then, the optimal horizontal position of the Hull Vane was found to be connected to the ship stern wave system. The Hull Vane in vertical direction should be positioned away from interacting with the ship hull. Bouckaert et al. (2015) studied on life-cycle cost analysis of offshore patrol vessel. Hull Vane has been applied for the speed value with the highest annual fuel consumption.

Firstly, the Hull Vane profile section and the horizontal position was optimized with the bare ship hull. In CFD studies for annual fuel consumption, struts and actuator disks were included to model real scenario. As a result of this study, annual fuel cost has been decreased by 12.5%. Bouckaert et al. (2015) have performed CFD studies on 108 m Holland Class OPV ship in terms of fuel consumption and seakeeping. The ship with and without Hull Vane was tested at 2 m and 4 m wave heights with a wave period of 8 s. Vertical acceleration on the stern area was decreased by 13.1% and 11.7% in 2 meters and 4 meters waves respectively.

The pitching motion was also reduced by 8.1% and 6.8%. The added resistance due to pitch and heave motion was decreased by 5.7% in 4-meter wave height and 4.9% in 2 meters' height. Uithof et al. (2016) investigated the Hull Vane effects on seakeeping of the ferries and ropax vessels. Both towing tank tests and CFD simulations were performed with and without Hull Vane. In towing tank tests, the period of roll motion has been lessened from 14.2 to 14.1 seconds. The natural period of pitch motion has been increased from 7.1 to 7.6 seconds. The added resistance value has

been decreased by 17.3% in regular waves with 2 meter heights (w = 0.55 rad/s). Similar results were obtained in CFD studies. Uithof et al. (2016) compared the influence of the Hull Vane, interceptors, trim wedges and ballasting systems on the 50 m Amecrc series patrol vessel by applying CFD techniques. Firstly, the position of the Hull Vane has been changed both at vertical and horizontal directions by keeping the span length constant. CFD studies were carried out without the struts of the Hull Vane because both the number of mesh would increase and had little effect on resistance. When the results were examined, it was seen that the position of Hull Vane in the vertical direction had a slight effect on the result. In comparison to Hull Vane and other trim control systems, it was observed that the Hull Vane was the most effective system in resistance and pitch motion. Another significant comparison study was carried out on Hull Vane versus lengthening of the ship hull by Hagemeister (2017). The total length of the ship increases with the installation of the Hull Vane. The purpose of this study was to compare the annual fuel consumption by increasing the ship's hull length by the same amount. As a result of the CFD simulations, the total annual fuel saving of Hull Vane installed ship was 15.1% while the length extended ship was calculated as 6.4%. In addition to the effects of Hull Vane on resistance and seakeeping, some unquantifiable contributions and benefits have been demonstrated by Uithof et al. (2016). These can be listed as reducing the size of the engine room, the initial investment costs with lower engine power, the size and costs of auxiliary machines connected to the main engine and tank volumes to create more usable space.

In this study, OpenFOAM 5 open source code was used to carry out CFD simulations, to investigate the Hull Vane effects on the total resistance and the resistance components of the ship in a calm water conditions. Besides the chord length of the Hull Vane has been changed by fixing the thickness to examine the sensitivity of the numerical study.

2 METHODOLOGY

2.1 *Ship model and Hull Vane configuration*

A motor yacht hull model in 16.5 scale is utilized for the experiments in this study. The length between perpendiculars (L_{BP}) of the model is 3.36 meters and the Froude number is 0.37. The main dimensions and the body plan of the model are given in Table 1 and Figure 1 respectively.

The NACA4412 hydrofoil which is broadly used in the literature has been selected for the Hull Vane cross section. The initial chord (c) length of the Hull Vane is 2% of the waterline length ($L_{WL} = 3.47$ m). Then the chord length of the Hull Vane has been changed by fixing the thickness of the Hull Vane. In CFD simulations, the leading edge of the Hull Vane has been fixed behind the transom of the ship model. Also, the attack angle has been kept at 0 degrees with respect to the calm waterline. The span length of the Hull Vane is equal to the ship model breadth. The Hull Vane configuration is shown in Figure 2. CFD simulations have been performed without the Hull Vane struts and the propellers of the ship model.

Table 1. Main dimensions.

Scale	16.5	Model	Ship
Length between perp.	L_{BP}(m)	3.358	55.4
Length on waterline	L_{WL}(m)	3.47	57.746
Breadth	B(m)	0.727	12
Draught (midship)	T(m)	0.212	3.5
Displacement volume	(m^3)	0.268	1204
Displacement _	(ton)	0.268	1234.1
Wetted surface area	W.S.A(m^3)	2.769	12439
Block coefficient	CB	0.533	0.533
Long. centre of buoyancy	L_{CB}(m)(+fwd)	−0.16	−2.636
Long. centre of floatation	LCF (m)(+fwd)	−0.348	−5.733
Service speed	V_S	2.15 m/s	17 knot

2.2 *Numerical modelling*

OpenFOAM is an open source library which is written in C ++ language. It has an extensive capacity to carry out different kind of fluid dynamics problems such as laminar, turbulent, multiphase flows. In this study, 3-D, incompressible, unsteady Navier-Stokes equations are solved by applying the finite volume method in order to calculate the resistance components of the ship model. The vector notation of the governing equations of the flow are given below; Newman (2018)

$$\nabla \mathbf{V} = 0, \tag{1}$$

$$\frac{\partial \mathbf{V}}{\partial t} + (\mathbf{V}\nabla)\mathbf{V} = -\frac{1}{\rho}\nabla \mathbf{p} + \nu \nabla^2 \mathbf{V} + \frac{1}{\rho}\mathbf{F}, \tag{2}$$

where V is the velocity, ρ is the fluid density, p is the mean pressure, $\nu = \mu/\rho$ is the kinematic viscosity coefficient, ∇ is the Laplace operator, F is the body force.

A typical two equation SST k-ω turbulence model is used to solve the eddy viscosity. k and ω represent the turbulence kinetic energy and the specific rate of dissipation respectively. The first order implicit (Euler) scheme is used to discretize the time. Gauss linear interpolation is used for finite volume discretization. PIMPLE algorithm, which is a combination of PISO (Pressure Implicit Split Operator) and SIMPLE (Semi Implicit Methods Pressure Linked Equations) algorithms, is used to solve pressure-velocity coupling. CFD simulations are carried out in two-phases, air and water. In addition, the pitch and heave motions of the ship model are released to model real scenario. Therefore, "interDymFoam" solver is used in

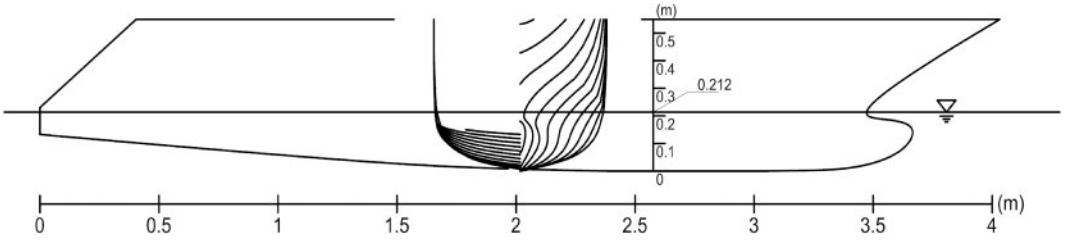

Figure 1. Body plan.

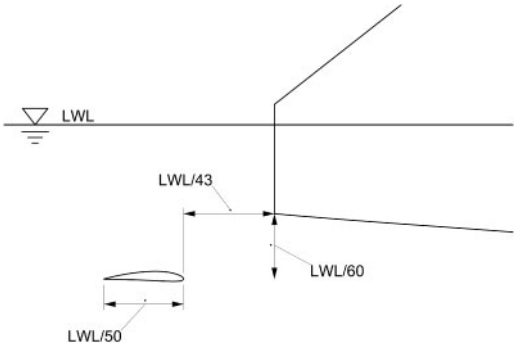

Figure 2. Hull Vane configuration.

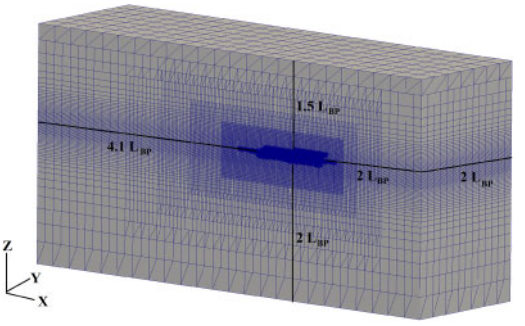

Figure 3. Computational domain and boundary distances.

Table 2. Boundary conditions according to the fluid properties and the turbulence parameters.

	Inlet	Outlet	Atmosphere	Hull
U	FV	OPMV	PIOV	MWV
p-rgh	FFP	ZG	TP	FFP
α. water	FV	VHFR	IO	ZG
k	FV	IO	IO	kqRWF
nut	FV	ZG	ZG	nutkRWF
omega	FV	IO	IO	omegaWF

OpenFOAM 5 library, which is "a solver for 2 incompressible, isothermal immiscible fluids using a VOF (volume of fluid) phase-fraction based interface capturing approach, with optional mesh motion and mesh topology changes including adaptive re-meshing".

The time step has been selected according to the ITTC (2011b) (International Towing Tank Conference) recommended procedures and guidelines. The recommended time interval is between 0.005 and 0.01 L/U seconds to accurately capture the flow features. In the validation and verification studies, the time step was chosen as a 0.005 second and the desired results were obtained.

2.3 *Computational domain and boundary conditions*

The inlet, bottom and side boundaries are located 2 L_{BP} away from the ship model and the outlet boundary is placed 4.1 L_{BP} downstream direction (see in Figure 3). These boundary distances are within the range specified in the ITTC procedure to avoid wave reflection from the boundaries.

Boundary conditions were determined according to ITTC guidelines. The ship model hull was specified by the wall function. The sides and the bottom boundaries were defined as the symmetry condition. Inlet, outlet and atmosphere boundary conditions were defined separately by considering the turbulence parameters and the flow characteristics. Detailed boundary conditions can be seen in Table 2.

In OpenFOAM, the Dirichlet boundary condition is represented by fixed value (FV). The Neumann boundary condition is expressed by zero gradient (ZG). The outlet phase mean velocity (OPMV) and pressure inlet outlet velocity (PIOV) applies zero gradient for outflow. The moving wall velocity corresponds to (MWV). The fixed flux pressure (FFP) sets the pressure gradient on the boundary by the velocity boundary condition. The total pressure (TP) is calculated by adding static and dynamic pressure components. The inlet outlet (IO) supplies a zero gradient outflow condition. The frequency, the kinetic eddy viscosity for roughness and the turbulence kinetic energy wall functions are represented by omegaWF, nutkRWF, kqRWF respectively. Islam, H. et al. (2018) have used the same boundary conditions to estimate the hydrodynamic derivatives of a container ship by using the OpenFOAM flow solver.

2.4 *Simulation mesh*

The domain mesh within determined boundary distances was created the with blockMesh utility in

Table 3. Spatial discretization uncertainty.

Number of mesh	Fine	2,503,279
	Medium	1,022,266
	Coarse	413,198
Refinement factor	r_{21}	1.348
	r_{32}	1.352
Total resistance coefficients	C_{T1}	0.00981
	C_{T2}	0.00982
	C_{T3}	0.01003
Apperant order	P_{last}	9.2304
Extrapolated value	$f_{ext;}21$	0.0098
Approximate relative error	(%) $e_{a;21}$	0.1306
Extrapolated relative error	(%) $e_{ext;21}$	0.0089
Fine grid convergence index	(%) $GCI_{fine;21}$	0.01

OpenFOAM. The topoSet was applied 5 times to increase the mesh density up to the ship model. There are two nested control volumes in order to capture the flow characteristics by refining the mesh around the free surface, bow and aft of the model ship. The snappyHexMesh utility was executed to create 3 dimensional meshes automatically from triangulated surface geometries such as Stereolithography (STL) or Wavefront Object (OBJ) format.

3 RESULTS AND DISCUSSION

3.1 *Verification and validation*

The spatial uncertainty estimation procedure in the CFD applications published by Celik et al. (2008) has been applied to bare ship model. The total mesh number of the fine, medium and coarse domains is 2.5 M, 1 M and 0.41 M respectively. The total resistance coefficients (C_T) obtained from CFD simulations were used as the variables. The spatial uncertainty calculation steps are shown in Table 3. According to uncertainty analysis, the fine grid convergence index (GCI) is 0.01%. Therefore, the CFD simulations for each case have been performed with the number of mesh used in the fine domain.

The towing tank experiments have been performed in Ata Nutku Ship Model Test Laboratory. The bare model hull CFD simulation has been carried out with fine domain mesh features at a design speed of 2.15 m/s. The experiment and the CFD simulation are compatible with each other and the total resistance coefficient (C_T) difference is 1.54%.

3.2 *Comparison of the resistance components*

It would be appropriate to rephrase the resistance components in order to examine the effect of Hull Vane on ship model resistance. Song, S. et al. (2018) investigated the effect of biofouling on ship hydrodynamic characteristics by comparing the ship resistance components. The total resistance (R_T) consists of two components: the frictional resistance (R_F) and the residuary resistance (R_R). The sum of the viscous pressure resistance (R_{VP}) and the wave making resistance (R_W) is equal to the residuary resistance (R_R).

$$R_T = R_F + R_{VP} + R_W, \tag{3}$$

The viscous pressure resistance (R_{VP}) is also proportional to the frictional resistance (R_F). This ratio is called form factor and is expressed as k.

$$R_{VP} = kR_F, \tag{4}$$

$$R_T = (1+k)R_F + R_W, \tag{5}$$

The total resistance and the resistance components can be expressed as dimensionless by dividing them with $(1/(2\rho SV^2))$. Here, ρ is the density of the water, S is the wetted surface area of the ship model and V is the design speed of the ship model.

$$C_T = C_F + C_R, \tag{6}$$

$$C_T = C_F + C_{VP} + C_W, \tag{7}$$

$$C_T = (1+k)C_F + C_W, \tag{8}$$

The coefficients of the total, frictional, viscous pressure and wave making resistance are represented as C_T, C_F, C_{VP} and C_W respectively.

In multi-phase CFD simulations, the frictional resistance and the residuary resistance coefficients are calculated separately to obtain the total resistance coefficient. The hull under the waterline of the ship model is simulated in a single phase (double body simulation), which gives the sum of the frictional resistance coefficient (C_F) and the viscous pressure coefficient (C_{VP}). In double body simulation, it should be emphasized that the forces on the transom of the ship model were not calculated. Since, it is completely dry in the multi-phase CFD simulations. Finally, the wave making resistance coefficient is obtained by subtracting the (C_F+C_{VP}) from the total resistance coefficient (C_T).

As shown in the Table 4, the total resistance coefficients with the resistance components of the ship model have been compared with and without the Hull Vane. The total wetted surface area has increased in the CFD analysis with the installation of the Hull Vane. Therefore, the frictional resistance of the ship model was expected to increase. CFD simulation results show good agreement with the expectations, showing the frictional resistance increment of 4.2%. It was observed that the viscous pressure resistance and wave making resistance have been decreased due to the presence of the Hull Vane. However, the wave making resistance constitutes a large percentage of the reduction in the total resistance. A negative pressure zone, which helps reducing the stern wave, appears on the top side of the Hull Vane due to accelerated flow from the aft geometry of the hull. The change in stern waves is shown in Figure 4 with and without the Hull Vane.

Table 4. Resistances components.

	10^3C_F	$10^3C_{V\,P}$	10^3C_W	10^3C_T
Bare Hull	3.20	0.91	5.70	9.81
Hull Vane (c70)	3.34	0.83	3.94	8.10
Difference (%)	+4.2	−8.9	−30.9	−17.4

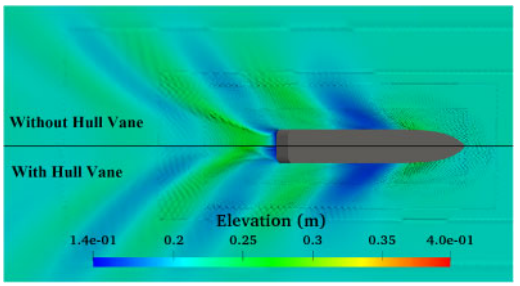

Figure 4. Wave elevation with and without Hull Vane.

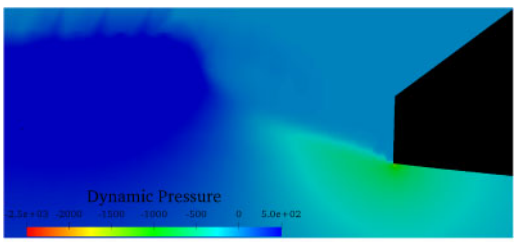

(a) Bare hull

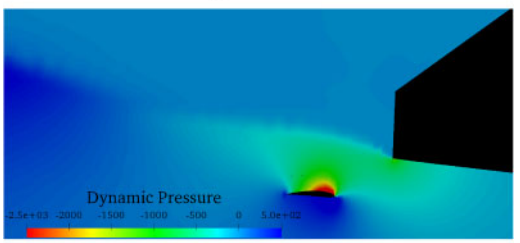

(b) With Hull Vane

Figure 5. Dynamic pressure distribution around the stern area.

Also, the pressure distribution of the stern profile section can be seen in Figure 5 (a) and (b). As a result, the wave making resistance and the total resistance have been decreased by 30.9 and 17.4% respectively on the model scale.

3.3 *Sensitivity of the numerical study*

The leading edge position, attack angle, maximum thickness and span length of the Hull Vane have been kept constant in all simulations. Different Hull Vanes with chord lengths of 1.73, 2, 2.3, 2.6, 2.9, 3.17 and 3.45% of the waterline length have been simulated at a design speed of 2.15 m/s. They are represented as

Table 5. Lengthened Hull Vane results.

	10^3C_F	10^3C_R	10^3C_T	Difference (%)
Bare Hull	3.20	6.61	9.81	–
c60	3.30	5.07	8.37	14.695
c70	3.34	4.77	8.10	17.387
c80	3.30	4.83	8.13	17.138
c90	3.29	4.76	8.06	17.884
c100	3.39	4.68	8.06	17.807
c110	3.25	4.52	7.77	20.805
c120	3.37	4.19	7.57	22.885

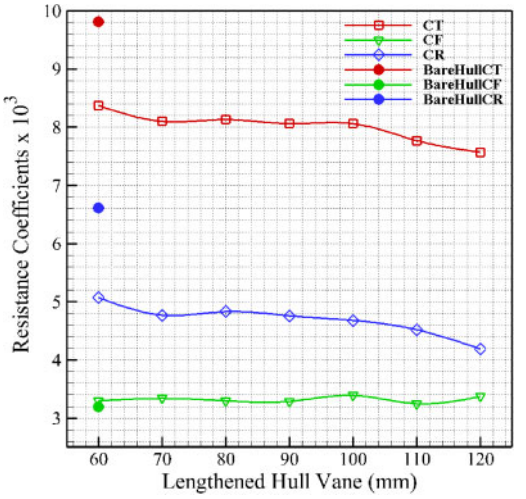

Figure 6. Lengthened Hull Vane resistance graph.

c60, c70, c80, c90, c100, c110 and c120 respectively in Table 5. The total resistance coefficient difference between the bare hull and the lengthened Hull Vane are also presented in Table 5. The resistance graph (in Figure 6) indicate that increasing the chord length of the Hull Vane, the residuary resistance (C_R) is monotonically decreasing whereas the frictional resistance (C_F) is non-monotonically slightly increasing.

4 CONCLUSIONS AND FUTURE WORK

The importance of the energy saving appendages has been increasing for not only the green environment but also the operating costs of the ships. The Hull Vane that is one of the energy saving systems, which is being implemented to the different type of vessels in order to decrease the power need of the ships. In this study, the impact of the Hull Vane on the ship resistance was examined in detail by using the OpenFOAM open source CFD code. It was observed that the CFD simulation results and the experiment results were consistent with each other for the bare hull. CFD simulations have been performed by the installation of the Hull Vane and it has been found that the total resistance of the ship model is decreased up to 22.9%.

A series of CFD analyses with the different chord lengths of the Hull Vane has been carried out to understand the effect on the ship total resistance. It was determined that the relative difference of the total resistance obtained for the different chord lengths of the Hull Vane was higher in the error caused by spatial numerical uncertainty. Therefore, this study constitutes a strong basis for the shape optimization of the Hull Vane.

In the future studies, full-scale and self-propelled CFD simulations will be performed with the optimized Hull Vane shape to investigate the impact of Hull Vane on real conditions.

ACKNOWLEDGEMENTS

High performance computing services have been provided free of charge by the National Centre of High Performance Computing (UHEM) unit at the Istanbul Technical University. I would like to thank Dr. Yigit Kemal Demirel and Dr. Tahsin Tezdogan for their help and guidance on CFD simulations at the University of Strathclyde. I also thank Mr. Can Nuri Özcan for his support in OpenFOAM.

REFERENCES

Bouckaert, B. et al. (2015). A life-cycle cost analysis of the application of a Hull Vane to an Offshore Patrol Vessel. *In 13th International Conference on Fast Sea Transport (FAST) Washington DC.*

Bouckaert, B. et al. (2015). Hull Vane on 108m Holland-Class OPVs: Effects on Fuel Consumption and Seakeeping. *In Proceeding of MAST Conference.*

Celik, I.B., Ghia, U. and Roache, P.J. (2008). Procedure for estimation and reporting of uncertainty due to discretization in CFD applications. *Journal of Fluids Engineering – Transactions of the ASME.*

Hagemeister, N (2017). Hull vane versus lengthening.

Islam, H. et al. (2018). Estimation of hydrodynamic derivatives of a container ship using PMM simulation in OpenFOAM. *Ocean Engineering. 164, 414–425.*

ITTC (2011b). Practical guidelines for ship CFD applications. *International Towing Tank Conference (ITTC).*

Newman, J. N. (2018). Marine hydrodynamics. *MIT press.*

Song, S. et al. (2018). An investigation into the effect of biofouling on the ship hydrodynamic characteristics using CFD. *Ocean Engineering. 175, 122–137.*

Uithof, K. et al. (2016). A cost-benefit analysis of Hull vane application on motor yachts.

Uithof, K. et al. (2014). An update on the development of the Hull Vane. *In 9th International Conference on High-Performance Marine Vehicles (HIPER) Athens.*

Uithof, K. et al. (2016). The Effects of the Hull Vane on Ship Motions of Ferries and RoPax Vessels. *RINA Design and Operation of Ferries and RoPax Vessels, London.*

Uithof, K. et al. (2016). A systematic comparison of the influence of the hull vane, interceptors, trim wedges, and ballasting on the performance of the 50M amecrc series 13 patrol vessels. *Proc. Warship 2016: Advanced Tech. Naval Design, Constr. Operation, Bath, UK.*